Theoretical Study of External Cavity Diode Laser Using Simulation of Modes

Dumanov E.V., Tronciu V.Z.,
Technical University of Moldova
Bd. Stefan cel Mare 168, MD-2004
Chisinau, Republic of Moldova

Dumanov E.V.
Institute of Applied Physics
Academy of Sciences of Moldova
Academiei Street 5, MD-2028
Chisinau, Republic of Moldova

Wenzel H.
Ferdinand-Braun-Institut, Leibniz-Institut für Höchstfrequenztechnik
Gustav-Kirchhoff Str. 4, 12489
Berlin, Germany

***Abstract* — This paper reports the results of numerical investigations of the modal behavior of a laser with an external feedback. The numerical calculations are based on the solution of the homogeneous coupled-wave equations using a transfer function approach. We showed that the number of laser modes is closely dependent on the material and device parameters as transmission and reflection coefficients of laser facets, length of active section etc.**

***Key words* — external cavity diode laser, simulation of modes.**

I. Introduction

During recent years semiconductor lasers under the influence of an external feedback have attracted attention due to its fundamental and applicative interest. A stabilized semiconductor diode subject to a proper external feedback with stable wavelength is required for various applications in spectroscopy, metrology, space communication etc. [1]. The stabilization of the wavelength can be achieved by a Bragg grating as external mirror. Recently, a new micro-integration approach was used to create a compact diode laser with a narrow linewidth and an external cavity for the application the quantum-optical precise experiments in space [2].

A simple model for simulation of the semiconductor laser with weak and moderate optical feedback was proposed by Lang-Kobayashi (LK) [3]. It constitutes a system of differential equations with delay. LK model allows a reasonable qualitative agreement with experiments and provides a good understanding of the nonlinear dynamics in this device [4]. LK approach has also been successfully used to obtain a good understanding of the stabilization or destabilization of the states of the continuous radiation on different configurations of the external cavity [5]. However, the LK model is mainly suitable for the study of laser optical system with a small and a large feedback relation to the length of the external cavity laser. In this case, the length of the emitter can be neglected. More appropriate way to describe the dynamics of semiconductor lasers with short external cavity is a traveling wave model. It represents a differential equation model, which includes the spatial distribution of fields [6, 7]. In this paper the eigensolutions (modes) and eigenvalues (frequencies) of the travelling wave model are calculated. Our paper is organized as follows. In the section II the basic equations is introduced. Section III is devoted to the computer simulation and analysis of the obtained results. Section IV contains the conclusions.

II. Basic Equations

We study a three-section external cavity diode laser. Its scheme is shown in Fig. 1. It consists of an active section with length L_1, an air gap with length L_2 and a passive section with length L_3. More details about the laser chip used for the active section can be found in [8].

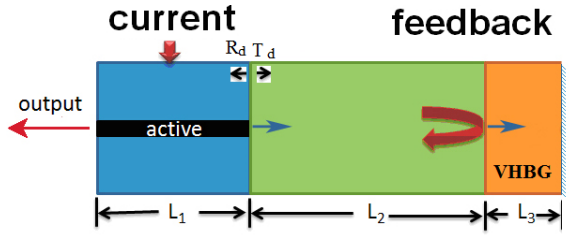

Fig. 1 Scheme of the external cavity diode laser. R_d and T_d are the reflection and transmission coefficients, respectively, at the facet of the laser chip towards the air gap [12].

The laser is described by the homogeneous coupled wave equations [6, 9, 10]

$$\begin{bmatrix} +\frac{\partial}{\partial z}+i\Delta\beta(z) & i\kappa^{+}(z) \\ i\kappa^{-}(z) & -\frac{\partial}{\partial z}+i\Delta\beta(z) \end{bmatrix}\begin{bmatrix} a(z) \\ b(z) \end{bmatrix}=0, \quad (1)$$

where

$$\Delta\beta(z,\lambda)=\beta(z,\lambda)-\beta_{\text{Bragg}} \quad (2)$$

is the relative complex propagation factor with

$$\beta_{\text{Bragg}} = \frac{N\pi}{\Lambda} \tag{3}$$

being the Bragg wave vector.
These equations are solved subject to homogeneous boundary conditions at $z = 0$

$$a(0) - r_0 b(0) = 0\,, \tag{4}$$

and at $z = L$

$$b(L) - r_L a(L) = 0, \tag{5}$$

where here r_0 is the reflectivity of the output facet ($z=0$) and r_L is the reflectivity of the rear plane of the VHBG ($z=L$).
The real part of the relative propagation factor (2) is expanded at the reference frequency $\omega_0 = 2\pi c / \lambda_0$, as follows

$$\Delta\beta(z,\lambda) = \text{Re}(\Delta\beta(z))\Big|_{\lambda_0} + \text{Re}\left(\frac{\partial\beta}{\partial\omega}\right)\Big|_{\lambda_0} \Omega + i\text{Imag}(\beta(z,\lambda))\,, \tag{6}$$

with Ω being the relative complex frequencies acting as eigenvalues to be determined. In what follows the equation (4) is set as an initial condition and (5) is numerically solved by Newton's method for given guess values of the relative complex frequencies.

The real part of the derivative of the relative propagation factor is given by

$$\text{Re}\left(\frac{\partial\beta}{\partial\omega}\right) = \frac{n_{\text{g}}(z)}{c}, \tag{7}$$

and as a result the relative propagation factor reads

$$\Delta\beta(z,\lambda) = \frac{2\pi}{\lambda}\Delta n(z,\lambda) + \frac{n_{\text{g}}(z)}{c}\Omega + \frac{i}{2}\left[g(z,\lambda) - \alpha_0(z)\right], \tag{8}$$

where n_g is the group index, Δn is the deviation of the phase index from the reference index, g is the gain and α_0 are the internal optical losses. In what follows the wavelength dependence of the gain is neglected.

The coupling coefficients are given by

$$\kappa^{\pm}(z) = \left[\kappa_{\text{r}}(z) + i\kappa_{\text{i}}(z)\text{e}^{\pm 2\pi i\phi_{\text{g}}(z)}\right]\text{e}^{\mp 2\pi i\phi(z)}, \tag{9}$$

where the imaginary part κ_i may be positive or negative (in-phase or anti-phase gain or loss grating, respectively). The phase ϕ can be used to model a phase shift of the grating along the cavity and the phase ϕ_{g} describes a phase shift between index and gain (loss) coupling.

The amplitude reflection coefficients are given by

$$r_0 = \sqrt{R_0}\,\text{e}^{2\pi i\phi_0} \quad , \; r_L = \sqrt{R_L}\,\text{e}^{-2\pi i\phi_L}\,, \tag{10}$$

where ϕ_0 and ϕ_L (in units 2π) can be used to describe the phases of the Bragg grating at the facets, i.e.

$$\phi_0 = \frac{N}{\Lambda}\Delta_0\,, \qquad \phi_L = \frac{N}{\Lambda}\Delta_L\,. \tag{11}$$

Here N is the order of the Bragg grating, Λ the period and Δ_0 and Δ_L are the exact positions of the facets relative to the Bragg grating.

At discontinuities $z = z_d$ the following transition condition is assumed:

$$\begin{bmatrix} a(z_d^{>}) \\ b(z_d^{>}) \end{bmatrix} = \frac{1}{t^{-}}\begin{bmatrix} t^{+}t^{-} - r^{+}r^{-} & r^{-} \\ -r^{+} & 1 \end{bmatrix}\begin{bmatrix} a(z_d^{<}) \\ b(z_d^{<}) \end{bmatrix}, \tag{12}$$

where $r^{\pm}$ and $t^{\pm}$ are the corresponding amplitude reflection and transmission coefficients, respectively.

Assuming section-wise constant $\Delta\beta$ and $\kappa^{\pm}$, Eq.(1) is solved by the transfer function [11]

$$\begin{bmatrix} a(z) \\ b(z) \end{bmatrix} = \begin{bmatrix} \cos(\gamma z) - i\Delta\beta\dfrac{\sin(\gamma z)}{\gamma} & -i\kappa^{+}\dfrac{\sin(\gamma z)}{\gamma} \\ +i\kappa^{-}\dfrac{\sin(\gamma z)}{\gamma} & \cos(\gamma z) + i\Delta\beta\dfrac{\sin(\gamma z)}{\gamma} \end{bmatrix}\begin{bmatrix} a(0) \\ b(0) \end{bmatrix}, \tag{13}$$

with

$$\gamma = \sqrt{(\Delta\beta)^2 - \kappa^{+}\kappa^{-}}\,. \tag{14}$$

It is well known that the imaginary part of the relative complex frequencies are the damping constants and the real part are the oscillation frequencies of the modes relative to the reference frequency. The threshold of a mode is reached, if for a certain gain (the threshold gain) in an active section the imagery part of the complex frequency (the damping constant) vanishes.
The wavelengths of the modes relative to the reference wavelength are given by

$$\Delta\lambda = \frac{d\lambda}{d\omega}\Big|_{\lambda_0}\,\text{Re}(\Omega). \tag{15}$$

For a Fabry-Perot laser ($\kappa^{\pm} = 0$) the system (1) can be analytically solved to obtain the relative complex frequencies

$$\mathrm{Re}(\Omega_m) = \frac{c}{\int_0^L n_g\, dz}\left[\pi\left(\frac{M+1}{2} - m\right) + \right.$$
$$\left. + \pi\,\mathrm{Int}\left(\frac{\int_0^L \mathrm{Re}(\Delta\beta)\, dz}{\pi}\right) - \int_0^L \mathrm{Re}(\Delta\beta)\, dz\right], \qquad (16)$$
$$\mathrm{Im}(\Omega_m) = -\frac{c}{\int_0^L n_g\, dz}\left[\frac{1}{2}\ln(|\, r_0 r_L\,|) + \int_0^L \mathrm{Im}(\beta(\lambda_m))\, dz\right],$$

where $m = 1, 2, 3, \ldots$ is the longitudinal mode index and M is the (odd) number of modes taken into account. These frequencies are the starting values of an embedding procedure where $\kappa^{\pm}$ and the reflection coefficients are stepwise changed to the original values.

III. Simulations

We consider an external cavity diode laser which operates at the wavelength $\lambda_0 = 0.78\ \mu\mathrm{m}$ (for more details see [12]). The reflection coefficient at the border between active region and air gap is R_d=*0.01* and between air gap and holographic volume Bragg grating is zero. The respective transmission coefficients are T_d = 0.8 and one. The active section length is L_1=1 mm, the air gap length L_2 = 30 mm, and the holographic volume Bragg grating length L_3 = 6 mm. Figure 2 shows a spectrum of the intensity reflection of the Bragg grating for $\kappa^{\pm} = 1.9\ \mathrm{cm}^{-1}$. The maximal field intensity reflection is 0.65.

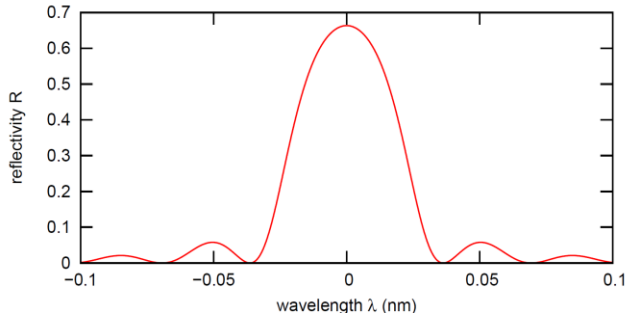

Fig. 2. Calculated reflectivity spectrum of the Bragg grating.

It is well known that to achieve a controlled stable generation of a single mode, we have to increase its gain margin with respect to the other modes, which in particular can be done by suitable design of the Bragg grating.

We begin our analysis for the given above parameters of the laser setup. Figure 3 shows the results of the numerical simulation for the relative threshold lasing frequency (top) and imaginary part of the frequency (bottom) as a function of the injected current. The decrease of the frequency with increasing current is caused by the increase of the effective index due to self-heating according to

$$\Delta n(I) = \frac{\partial n}{\partial I}\Delta I \quad \text{with} \quad \frac{\partial n}{\partial I} = 10^{-5}\ \mathrm{mA}^{-1}.$$

If the detuning between the frequency of the mode and the constant Bragg frequency is too large, the lasing mode jumps back to a longitudinal mode having a higher frequency. As mentioned above Figure 3 (bottom) shows the imaginary part of the frequency as a function of the injected current. From this figure it is possible to find for a given current the dominant mode characterized by a vanishing imaginary part of the frequency.

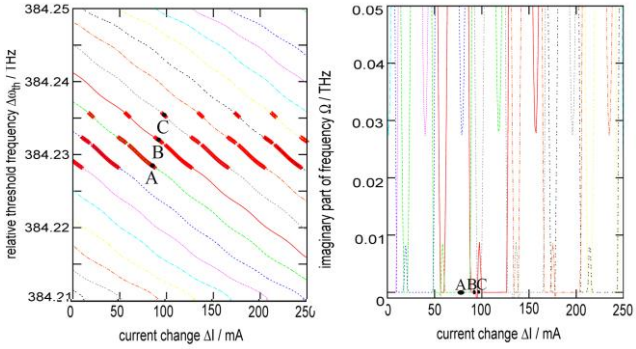

Fig. 3. The relative threshold lasing frequency as a function of the injected current (top) and imaginary part of frequency as a function of the injected current (bottom).

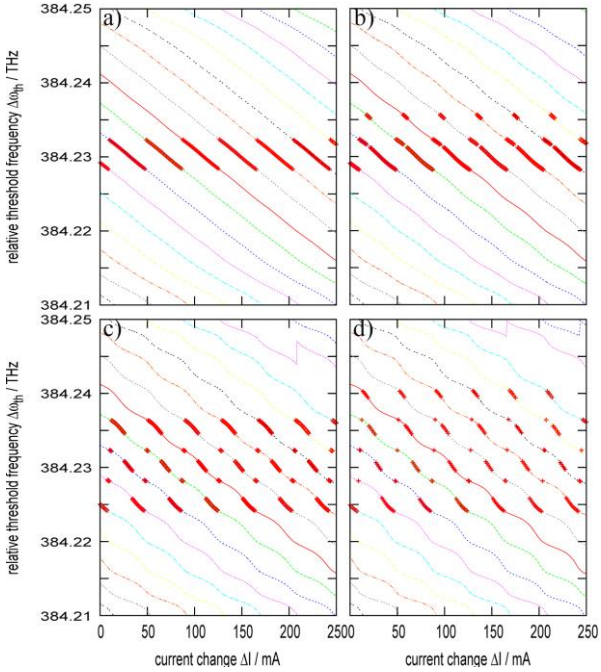

Fig. 4. The relative threshold lasing frequency as a function of the injected current for different values of the amplitudes reflectivity R_d at the border between active region and airgap a) R_d=0.001, b) R_d = 0.01, c) R_d = 0.05 and d) R_d = 0.1. Thick lines represent the main dominant optical mode. Thin lines show the all CW states for the maximal field intensity reflection 0.7. Other parameters are as follows: T_d=0.8, L_1=1 mm, L_2 =30 mm, L_3 = 6 mm.

In what follows, we vary the transmission and reflection coefficients. Figure 4 shows the case when we change the reflection coefficient R_d keeping constant the value 0.8 of the transmission coefficient. Let consider the lower value of the reflection coefficient R_d =0.001. Figure 4a shows that only two modes are involved in the jumps. On the other hand, when

we increase the reflection coefficient, as shown in Fig. 4(c-d), the laser behavior become more complex and more modes are involved in the lasing.

Now we consider what is predicted to happen if we change the length of the air gap keeping constant the transmission coefficient (T_d =0.8), the reflectivity (R_d = 0.01), the length of the active section (L_1=1 mm), and the length of Bragg grating section (L_3 = 6 mm). When we increase the length of air gap section more external cavity modes are involved in the jumps (see Fig. 5). On the other hand, it is well known the short length of air gap section reduces the number of modes involved in the jumps and laser will operate in the single mode regime.

Another important laser characteristic is the longitudinal power profile shown in Figure 6. Letters 'A', 'B' and 'C' represent different modes from Figure 3. The total value of the power consists of a forward and a backward travelling component.

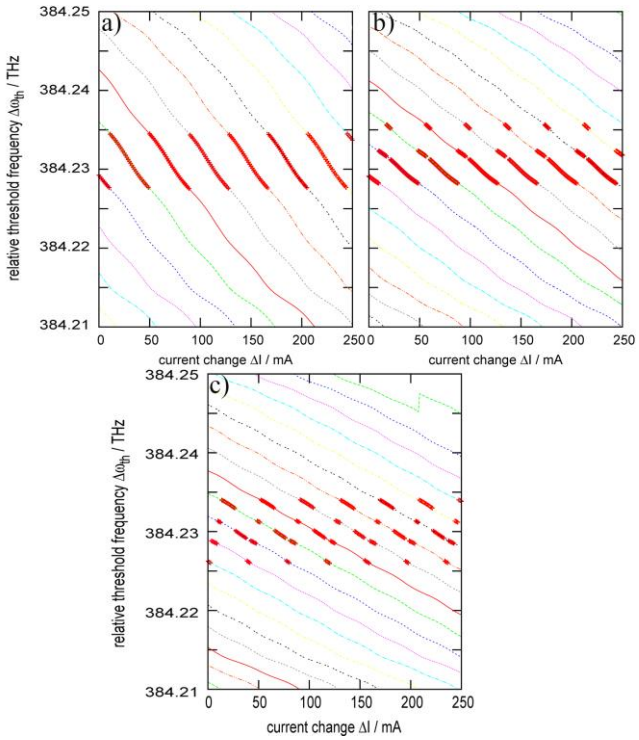

Fig. 5. The relative threshold lasing frequency as a function of the injected current for different values of the length of airgap: a) L_2 = 15 mm, b) L_2 = 30 mm, and c) L_2 = 45 mm. Thin lines show the all CW states for the maximal field intensity reflection 0.7. Other parameters are as follows: R_d=0.01, T_d=0.8

The first small region defines the active section of the laser where the forward and a backward travelling components are being amplified. The second section of the laser (air gap) is characterized by a linear transmission without changing power. The third region is the Bragg grating where the power varies exponentially. Fig. 6(A) shows the power profiles in the laser close to the jump point to another mode with a higher frequency. Fig 6(B) shows the power profiles when the mode just made the jump. Therefore, the total power in the air gap is greater than the previous Fig. 6 (A). Figure 6(C) shows the power profiles when mode makes an extra jump. In this case the total power will be less than in cases represented on the Fig. 6(A) and Fig. 6(B), because the mode originates from a former chip mode.

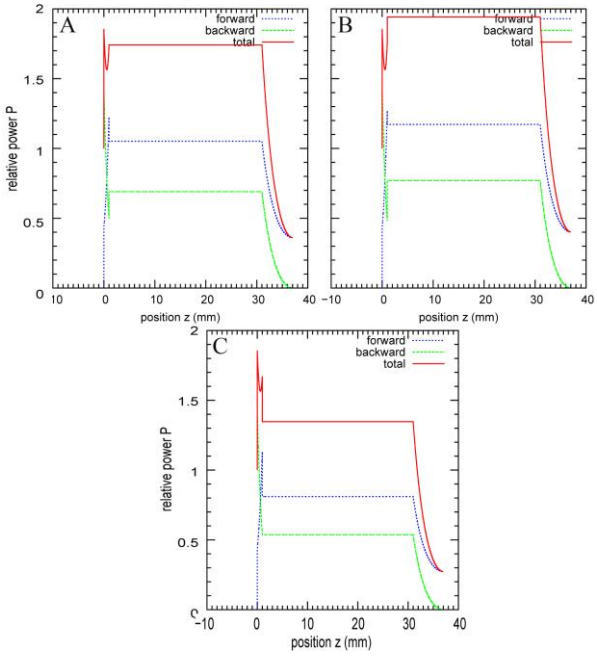

Fig. 6. The relative power P as function of the position z. Solid line is a total relative power, dotted line is the forward component, and dashed line is the backward component.

CONCLUSIONS

We studied a three section diode laser using a calculation based on the solution of the homogeneous coupled-wave equations with a transfer function approach. The lasing wavelengths as function of the increased injected current and the relative power P as function of the position z were obtained. It was showed that the number of lasing modes is closely dependent on the air gap length, transmission and reflection coefficients at the interface sections. Thus, reduction of transmission coefficient and increase of the reflection coefficient leads to the formation of the secondary cavity, and vice versa, increase of the transmission coefficient and decrease of the reflection coefficient leads to the stable single-mode lasing. There is a similar dependence of the number of modes involved in the jumps on the length of the air gap section. If we increase the length of the air gap section more modes are involved in the jumps of modes. And inversely, if we decrease the length of air gap section only two modes are involved in the jumps.

ACKNOWLEDGMENT

This work has been supported by the Academy of Sciences of Moldova and Federal Ministry of Education and Research of Germany (BMBF) (Grant no. 13.820.05.08/GF), STCU -5993.

REFERENCES

[1] D. Aguilera, H. et al "STE-QUEST-test of the universality of free fall using cold atom interferometry". Class. Quantum Grav., vol. 31, 115010 (**2014**); B. J. Bloom, et al. "An optical lattice clock with accuracy and stability at the 1018 level". Nature, vol. 506, 71, (**2014**); T. Sodnik, B. Furch, and H. Lutz. "Optical Intersatellite Communication". IEEE J. Select. Top. Quant. Electron.. vol. 16, 1051, (**2010**)

[2] E. Luvsandamdin, S. Spießberger, M. Schiemangk, A. Sahn, G. Mura, A. Wicht, A. Peters, G.Erbert, and G.Tränkle. "Development of narrow linewidth, micro-integrated extended cavity diode lasers for quantum optics experiments in space". Appl. Phys. B, vol. 111(2), 255, (**2013**)

[3] R. Lang and K. Kobayashi. "External optical feedback effects on semiconductor injection laser properties". IEEE J. Quantum Electron., vol. 16, 347, (**1980**)

[4] D. Lenstra, G. Vemuri, and M. Yousefi. in "Unlocking dynamical diversity: Optical feedback effects on semiconductor laser", D. M. Kane, and K. A. Shore, Editors, John Wiley Sons, west Sussex, (**2005**), Chapter: Generalized optical feedback: Theory, pp. 55 - 80

[5] V. Z. Tronciu, H. -J. Wünsche, M. Wolfrum and M. Radziunas. "Semiconductor laser under resonant feedback from a Fabry-Perot resonator: Stability of continuous-wave operation". Phys. Rev. E, vol. 73, 046205, (**2006**)

[6] U. Bandelow, M. Radziunas, J. Sieber, and M. Wolfrum. "Impact of gain dispersion on the spatio-temporal dynamics of multisection lasers". IEEE J. Quantum Electron., vol. 37(2), 183, (**2001**)

[7] M. Radziunas, K. - H. Hasler, B. Sumpf, T. Q. Tien, H. Wenzel. "Mode transitions in distributed bragg reflector semiconductor lasers: experiments, simulations and analysis". J. Phys. B: At. Mol. Opt. Phys., vol. 44, 105401, (**2011**)

[8] H. Wenzel, K. Hausler, G. Blume, J. Fricke, M. Spreemann, M. Zorn, and G. Erbert. "High-power 808 nm ridge-waveguide diode lasers with very small divergence, wavelength-stabilized by an external volume Bragg grating". Optics Lett., vol. 34, 1627, (**2009**)

[9] H. - J. Wünsche, U. Bandelow, H. Wenzel. "Calculation of combined lateral and longitudinal spatial hole burning in λ/4 shifted DFB lasers". IEEE J. Quantum Electronics, vol. 29(6), 751, (**1993**)

[10] H. Wenzel, U. Bandelow, H. - J. Wünsche, J. Rehberg. "Mechanisms of fast self pulsations in two-section DFB lasers". IEEE J. Quantum Electronics, vol. 3**2**(1), 69, (**1996**)

[11] U. Bandelow, U. Leonhardt. "Light propogation in one-dimensional lossless dielectrica: transfer matrix method and coupled mode theory". Optics Communication, vol. 101(1–2), 92, (**1993**)

[12] M. Radziunas, V. Z. Tronciu, E. Luvsandamdin, C. Kürbis, A. Wicht, H. Wenzel. "Study of Microintegrated External-Cavity Diode Lasers: Simulations, Analysis, and Experiments". IEEE J. Quantum Electronics, vol. 51, 2000408 (**2015)**